

Spatial electron-spin splitting in single-layered semiconductor microstructure modulated by Dresselhaus spin-orbit coupling

Jia-Li Chen(陈嘉丽), Sai-Yan Chen(陈赛艳), Li Wen(温丽), Xue-Li Cao(曹雪丽), and Mao-Wang Lu(卢卯旺)

Citation: Chin. Phys. B, 2024, 33 (**11**): 118501. DOI: 10.1088/1674-1056/ad6b83
Journal homepage: http://cpb.iphy.ac.cn; http://iopscience.iop.org/cpb

What follows is a list of articles you may be interested in

Fully spin-polarized, valley-polarized and spin-valley-polarized electron beam splitters utilizing zero-line modes in a three-terminal device

Xiao-Long Lü(吕小龙), Jia-En Yang(杨加恩), and Hang Xie(谢航)
Chin. Phys. B, 2024, 33 (**6**): 068502. DOI: 10.1088/1674-1056/ad2609

Influence of exchange bias on spin torque ferromagnetic resonance for quantification of spin-orbit torque efficiency

Qian Zhao(赵乾), Tengfei Zhang(张腾飞), Bin He(何斌), Zimu Li(李子木), Senfu Zhang(张森富), Guoqiang Yu(于国强), Jianbo Wang(王建波), Qingfang Liu(刘青芳), and Jinwu Wei(魏晋武)
Chin. Phys. B, 2024, 33 (**5**): 058502. DOI: 10.1088/1674-1056/ad2d55

Interfacial DMI in Fe/Pt thin films grown on different buffer layers

Wen-Jun Zhang(张文君), Fei Wei(魏菲), Bing Liu(刘冰), Yang Zhou(周阳), Shi-Shou Kang(康仕寿), and Bing Sun(孙兵)
Chin. Phys. B, 2024, 33 (**4**): 048501. DOI: 10.1088/1674-1056/ad1b41

Valleytronic topological filters in silicene-like inner-edge systems

Hang Xie(谢航), Xiao-Long Lü(吕小龙), and Jia-En Yang(杨加恩)
Chin. Phys. B, 2024, 33 (**1**): 018502. DOI: 10.1088/1674-1056/ad0714

Method of simulating hybrid STT-MTJ/CMOS circuits based on MATLAB/Simulink

Min-Hui Ji(冀敏慧), Xin-Miao Zhang(张欣苗), Meng-Chun Pan(潘孟春), Qing-Fa Du(杜青法), Yue-Guo Hu(胡悦国), Jia-Fei Hu(胡佳飞), Wei-Cheng Qiu(邱伟成), Jun-Ping Peng(彭俊平), Zhu Lin(林珠), and Pei-Sen Li(李裴森)
Chin. Phys. B, 2023, 32 (**7**): 078506. DOI: 10.1088/1674-1056/acad69

Spatial electron-spin splitting in single-layered semiconductor microstructure modulated by Dresselhaus spin–orbit coupling

Jia-Li Chen(陈嘉丽), Sai-Yan Chen(陈赛艳)[‡], Li Wen(温丽), Xue-Li Cao(曹雪丽), and Mao-Wang Lu(卢卯旺)[†]

College of Physics and Electronic Information Engineering, Guilin University of Technology, Guilin 541004, *China*

(Received 19 May 2024; revised manuscript received 1 August 2024; accepted manuscript online 6 August 2024)

Combining theory and computation, we explore the Goos–Hänchen (GH) effect for electrons in a single-layered semiconductor microstructure (SLSM) modulated by Dresselhaus spin–orbit coupling (SOC). GH displacement depends on electron spins thanks to Dresselhaus SOC, therefore electron spins can be separated from the space domain and spin-polarized electrons in semiconductors can be realized. Both the magnitude and sign of the spin polarization ratio change with the electron energy, in-plane wave vector, strain engineering and semiconductor layer thickness. The spin polarization ratio approaches a maximum at resonance; however, no electron-spin polarization occurs in the SLSM for a zero in-plane wave vector. More importantly, the spin polarization ratio can be manipulated by strain engineering or semiconductor layer thickness, giving rise to a controllable spatial electron-spin splitter in the field of semiconductor spintronics.

Keywords: semiconductor spintronics, single-layered semiconductor microstructure (SLSM), spin–orbit coupling (SOC), Goos–Hänchen (GH) effect, electron-spin polarization

PACS: 85.75.–d, 72.80.Ey, 71.70.Ej, 72.25.Dc **DOI:** 10.1088/1674-1056/ad6b83

1. Introduction

Unlike in existing semiconductor devices, in spintronics devices digital information '0' and '1' is encoded by electron spins.[1] However, this encoding scheme cannot be realized by utilizing conventional semiconductors owing to the spin degeneracy of electron states.[2] The generation and control of spin-polarized electrons in traditional semiconductors are critical issues in semiconductor spintronics.[3] In general, either the Zeeman effect[4] or spin–orbit coupling (SOC)[5] can be employed to achieve spin polarization of electrons in ordinary semiconductors, as both these mechanisms can effectively remove spin degeneracy from semiconductors.[6] Based on these principles, some effective methods for realizing spin polarization have been proposed, for example injecting highly spin-polarized electrons into semiconductors from magnetic materials,[7] producing magnetic semiconductors, such as diluted magnetic semiconductor,[8] and reasonably utilizing various quantum effects in semiconductor microstructures such as spin filtering,[9] spatial spin splitting[10] and temporal spin filtering.[11]

Recently, the creation and manipulation of spin polarization by the spin filtering effect has received much attention for electrons in layered semiconductor microstructures (LSMs).[12] Resorting to modern materials growth technology, such as molecular beam epitaxy[13] and metal organic chemical vapor deposition,[14] LSMs can be obtained by assembling micro-thick semiconductors along the direction desired in experiments. In a LSM, structure inversion symmetry is broken, which makes electron spins interact with the spatial motion, i.e., SOC appears. There are usually two different types of SOC: Rashba and Dresselhaus types. Rashba SOC comes from structural inversion asymmetry induced at interfaces or surfaces, and its strength can be controlled by an external electric field;[15] Dresselhaus SOC, with a strength that is tunable by strain engineering, originates from bulk inversion asymmetry.[16] These valuable types of SOC can effectively remove spin degeneracy of electrons from semiconductors, induce zero-field spin splitting and create an electron-spin polarization effect, giving LSMs great potential for applications in semiconductor spintronics devices.[17]

Selecting the semiconductor InSb, He *et al.*[18] and Lu *et al.*[19] theoretically explored the spin filtering effect for electrons in single-layered semiconductor microstructures (SLSMs). Either Rashba SOC or Dresselhaus SOC was found to create evident spin filtering; however, their contribution to electron-spin polarization was not equivalent. In addition, the spin polarization ratio depends on the electron energy, the in-plane wave vector and the incident direction. In particular, both the magnitude and sign of the spin polarization ratio can be manipulated by an externally applied electric field, strain engineering and semiconductor layer thickness. Based on such a SLSM, a tunable electron-spin filter was obtained. Combining InSb and GaSb, Lu *et al.*[20,21] investigated the Rashba and Dresselhaus SOC-induced spin filtering effect and spin polarization for electrons in a double-layered semiconductor microstructure and a corresponding electron-spin fil-

[†]Corresponding author. E-mail: maowanglu@glut.edu.cn
[‡]Corresponding author. E-mail: sychen02@126.com

© 2024 Chinese Physical Society and IOP Publishing Ltd

ter device was achieved. Assembling InSb, $In_xGa_{1-x}As$ and GaSb, Cao *et al.*[22,23] proposed a three-layered semiconductor microstructure and investigated the electron-spin filtering effect. They further explored the influence of δ-doping[24,25] and found that electron-spin filtering can be controlled by changing the weight or position of δ-doping, leading to a structurally manipulable electron-spin filter. The impact of an applied bias on the spin filtering effect in this LSM was studied and an electrically controllable electron-spin filter was developed theoretically.[26] Motivated by the above research, in the present work we theoretically explore the Goos–Hänchen (GH) effect for electrons in a SLSM modulated by Dresselhaus SOC. Due to the wave nature of light, a light beam totally reflected at an interface between dielectric media undergoes a lateral shift from the position predicted by geometrical optics, known as the GH effect.[10] Because of the quantum mechanical nature of the wave, the GH effect also occurs for electrons traversing a SLSM. It was found that GH displacement of electrons across a SLSM depends obviously on spins thanks to Dresselhaus SOC. As a result, electron spins can be separated in the space dimension by the spin-related GH shift and a spin polarization effect appears in the SLSM. Moreover, the spin polarization ratio is tunable by the lattice strain or semiconductor layer thickness. Based on these interesting findings, a controllable spatial electron-spin splitter (SESS) is proposed for the field of semiconductor spintronics.

2. Theory and method

Figure 1 schematically shows a GaSb-based SLSM, a structural model and GH displacement of electrons. Here, the semiconductor layer grows along the z direction, while the coordinates (x, y, z) are assumed to be parallel to the cubic crystal axes ([100], [010], [001], respectively). The physical parameters d and V are semiconductor layer thickness and the equivalent potential of electrons in GaSb, m, α and $k_\parallel = \sqrt{k_x^2 + k_y^2}$ represent mass, incidence angle and in-plane wave vector of an electron and $S_\uparrow$ and $S_\downarrow$ are the GH displacements for spin-up and spin-down electrons, respectively. Note that the incidence angle is related to the momentum or wave vector through the relationship $k_\parallel = k\sin\alpha$, where $k = \sqrt{k_\parallel^2 + k_z^2}$ is the wave vector of electrons. In the framework of the effective mass approximation, the Hamiltonian for an electron in this SLSM reads

$$H = -\frac{\hbar^2}{2m^*}\frac{\partial^2}{\partial z^2} + \frac{(\hbar k_\parallel)^2}{2m^*} + V + \eta_D(\sigma_x k_x - \sigma_y k_y)\frac{\partial^2}{\partial z^2}, \quad (1)$$

where m^*, η_D and $\sigma = (\sigma_x, \sigma_y, \sigma_z)$ stand for effective mass, Dresselhaus SOC strength and the Pauli vector, respectively. Taking spin quantization z-axis, the above Hamiltonian can be diagonalized by

$$H = -\frac{\hbar^2}{2m^*}\left(1 - \frac{2m^*}{\hbar^2}\sigma_z\eta_D k_\parallel\right)\frac{\partial^2}{\partial z^2} + \frac{(\hbar k_\parallel)^2}{2m^*} + V, \quad (2)$$

where $\sigma_z = +1/-1$ or $\uparrow/\downarrow$ stands for spin-up/-down electrons. For convenient numerical calculation, all involved quantities are undimensionalized, such as $E \to EE_0$ and $x \to x\ell_0$, where E_0 and $\ell_0 = \hbar/\sqrt{mE_0}$ are basic units of energy and length, respectively, for example $\ell_0 = 0.86$ nm for $E_0 = 0.1$ eV. Because electrons are free in the semiconductor-layer plane in the SLSM, the electron wave function is expressed by $\Phi(x,y,z) = e^{ik_\parallel \cdot r}\psi(z)$, where $r = (x,y)$ and $\psi(z)$ are the position vector in the semiconductor-layer plane and the z-component of the wave function. Substituting the stationary Schrödinger equation $H\Phi = E\Phi$ with electron energy E, we have

$$-\frac{\hbar^2}{2m^*_{\sigma_z}}\psi''(z) + U_{\text{eff}}(V,d,k_\parallel)\psi(z) = E\psi(z), \quad (3)$$

where $m^*_{\sigma_z} = (\frac{m}{m^*} - 2\sigma_z\eta_D k_\parallel)^{-1}$ and $U_{\text{eff}}(V,d,k_\parallel) = \frac{mk_\parallel^2}{2m^*} + V$ can be viewed as spin-dependent effective mass and the effective potential experienced by electrons in the SLSM device, respectively.

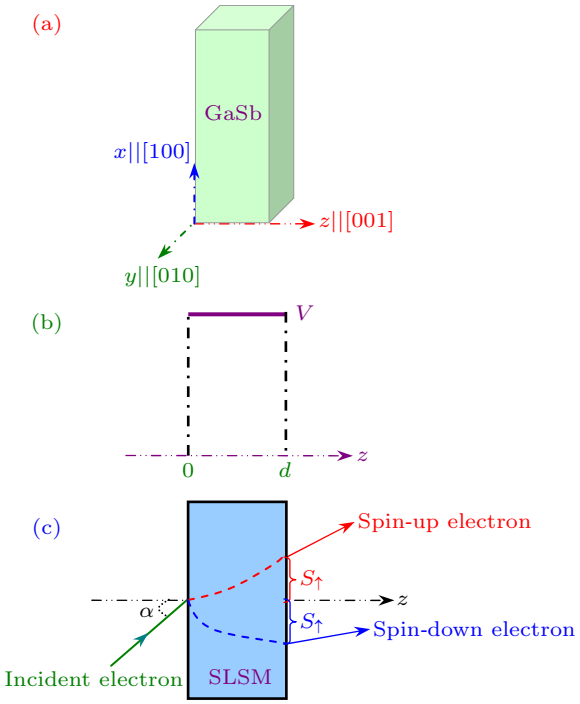


Fig. 1. (a) GaSb-based SLSM growing along the $z\|[001]$ direction, (b) physical model and (c) GH shift for electron across the SLSM, where d is the layer thickness, V means the equivalent potential of electron in semiconductor, $S_{\uparrow/\downarrow}$ represents spin-related GH displacement and α stands for the incident angle.

We utilize the improved transfer matrix method[27] to exactly solve the Schrödinger equation (3) of electrons in the SLSM. Wave functions for electrons in incident and outgoing regions can be written by $\psi_{\text{in}}(z) = \exp(ik_l z) + \gamma\exp(-ik_l z)$, $z < 0$ and $\psi_{\text{out}}(z) = \tau\exp(ik_r z)$, $z > d$, respectively, where $k_l =$

$k_{\rm r}=\sqrt{2E-k_{\parallel}^2}$ and γ/τ stands for the reflection/transmission amplitude. In this SLSM device, the wave function of electrons is $\psi(z)=C\exp(\mathrm{i}kz)+D\exp(-\mathrm{i}kz)$, $0<z<d$, where

$$k=\sqrt{2(m^*/m)(E-V-\sigma_z\eta_{\rm R}k_{\parallel}-k_{\parallel}^2)}$$

and C/D is pending constant. In light of the continuity of these wave functions at boundaries ($z=0$, d), one readily gets

$$\begin{pmatrix}1 & 1\\ \mathrm{i}k_{\rm l} & -\mathrm{i}k_{\rm l}\end{pmatrix}\begin{pmatrix}1\\ \gamma\end{pmatrix}=M\begin{pmatrix}\mathrm{e}^{\mathrm{i}k_{\rm r}d} & \mathrm{e}^{-\mathrm{i}k_{\rm r}d}\\ \mathrm{i}k_{\rm r}\mathrm{e}^{\mathrm{i}k_{\rm r}d} & -\mathrm{i}k_{\rm r}\mathrm{e}^{-\mathrm{i}k_{\rm r}d}\end{pmatrix}\begin{pmatrix}\tau\\ 0\end{pmatrix}, \quad (4)$$

where

$$M=\begin{pmatrix}\cos(kd) & -\sin(kd)/[k(m^*/m-2\sigma_z\eta_{\rm D}k_{\parallel})]\\ [k(m^*/m-2\sigma_z\eta_{\rm D}k_{\parallel})]\sin(kd) & \cos(kd)\end{pmatrix}$$

is known as the transfer matrix. Implicitly solving for Eq. (4), we get a transmission wave amplitude $\tau=2k_\ell/w$, where $w=|w|\exp(\mathrm{i}\phi)$ is a complex number and ϕ is also the phase shift for electrons traversing the SLSM. According to the stationary phase method,[28] GH displacement for electrons across the SLSM device as presented in Fig. 1 can be calculated by

$$S_{\sigma_z}(E,k_{\parallel},\eta_{\rm D})=\left.\frac{\partial\phi}{\partial k_{\parallel}}\right|_E. \quad (5)$$

The degree of the spin polarization effect for electrons in the SLSM device can be characterized in the so-called spin polarization ratio as[10]

$$P_{\rm S}(E,k_{\parallel},\eta_{\rm D})\equiv S_{\uparrow}-S_{\downarrow}, \quad (6)$$

where $S_{\uparrow}$ and $S_{\downarrow}$ stand for GH displacements for spin-up and spin-down electrons across the SLSM device, respectively.

3. Results and discussion

The partial physical quantities for our considered semiconductor GaSb are $m^*=0.041m$, $V=0.52$ eV and $\eta_{\rm D}=0.187$ eV·nm^3.[29] To begin with, in Fig. 2 the GH displacement (S_{σ_z}) as the function of the incident energy (E) is presented for spin-up (up-triangle curve) and spin-down (down-triangle curve) electrons traversing the GaSb-based SLSM device as indicated in Fig. 1, where $k_y=0.4$ nm^{-1}, $d=6.0$ nm, $V=0.52$ eV, and $\eta_{\rm D}=0.187$ eV·nm^3. For the calculated energy range, negative GH shifts can be observed clearly for both spin-up and spin-down electrons across the SLSM device. Moreover, GH displacement of spin-down electrons is larger and shifts to the high-energy direction with increasing electron energy compared with that of spin-up electrons. Therefore, an evident difference in GH shifts between spin-up and spin-down electrons appears in the SLSM device. Clearly, this discrepancy of GH displacement stems from Dresselhaus SOC since the SOC can effectively remove spin degeneracy of electrons from semiconductor materials. At the same time, this also implies that the electron-spin polarization effect can be realized by separating spins in the space dimension utilizing spin-related GH shifts for electron across the SLSM device. Additionally, when the incident energy is approximately 0.68 eV, GH displacement reaches a maximum. This can be understood by the resonance, i.e., when the incident energy is exactly equal to the bound energy level, which can be obtained by solving the Schrödinger equation for electrons in the SLSM device.

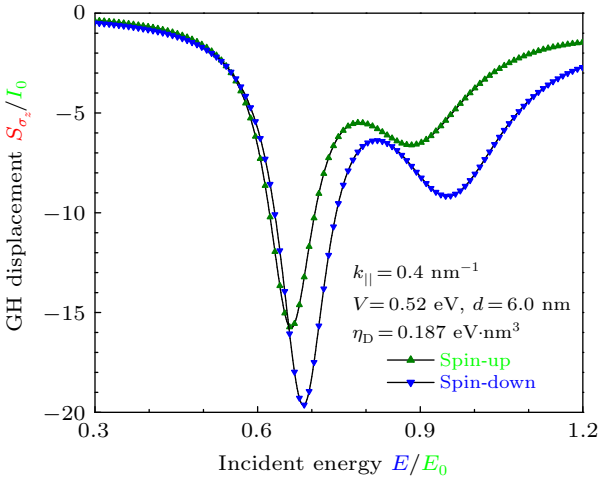


Fig. 2. GH displacement varies with incident energy for spin-up (▲-curve) and spin-down (▼-curve) electrons in the SLSM device, where equivalent potential, in-plane wave vector, Dresselhaus-SOC strength and semiconductor-layer thickness are $V=0.52$ eV, $k=0.4$ nm^{-1}, $\eta_{\rm D}=0.187$ eV·nm^3, and $d=6.0$ nm, respectively.

In Fig. 3, we show the variation of the spin polarization ratio ($P_{\rm S}$) with incident energy (E) for in-plane wave vector $k_{\parallel}=0$ nm^{-1} (squares), 0.2 nm^{-1} (circles), and 0.4 nm^{-1} (stars), respectively, where other physical parameters are chosen to be identical to those in Fig. 2. It is true that an evident electron-spin polarization effect can be observed clearly. Nevertheless, no spin polarization effect occurs in the SLSM device for a zero in-plane wave vector (i.e., the normal incidence), which is because the Hamiltonian (1) of an electron in the SLSM is now unrelated to the spins. When increasing in-plane wave vector, the electron-spin polarization effect becomes stronger. Moreover, the spin polarization ratio reaches its maximum and alters its sign at the resonance, for example for $k_{\parallel}=0.4$ nm^{-1} (stars) resonance occurs at $E\approx0.63$ eV.

This anisotropy of the spin polarization effect pertaining to the in-plane wave vector is attributed to the $k_{\|}$-dependence of both the effective potential (U_{eff}) and the spin-related effective mass ($m^*_{\sigma_z}$).

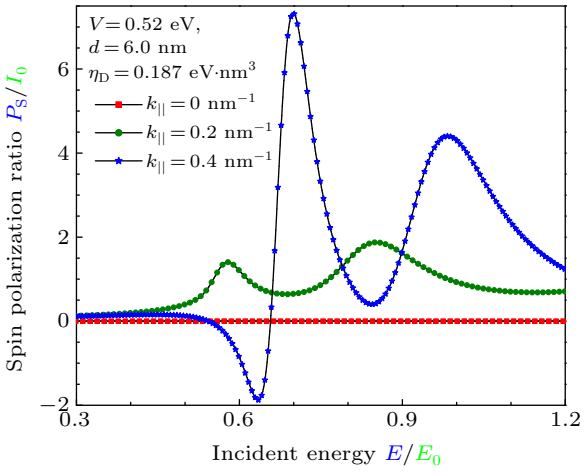


Fig. 3. Spin polarization ratio changes with the incident energy for in-plane wave vector $k_{\|}=0.0$ nm^{-1}, 0.2 nm^{-1}, and 0.4 nm^{-1}, where other physical parameters are the same as those in Fig. 2.

So far, one can conclude that the GaSb-based SLSM, as plotted in Fig. 1, can be designed as an effective SESS device and is an excellent spin-polarized source for semiconductor spintronics device applications. As we all know, a controllable spin-polarized source is particularly important in semiconductor spintronics.[30] In the following, we investigate how to manipulate the SLSM GaSb-based SESS device in order to obtain a tunable spin-polarized source for semiconductor spintronics devices. The effective potential (U_{eff}) of electrons in the GaSb-based SLSM is dependent on the strength of Dresselhaus SOC (η_D) modulated by strain engineering. This SESS device can therefore be controlled by strain. In Fig. 4 we present the spin polarization ratio (P_S) versus electron energy (E) for a Dresselhaus SOC strength of $\eta_D = 0.187$ eV·nm^3 (squares), 0.287 eV·nm^3 (circles), and 0.387 eV·nm^3 (stars), where $k_{\|}=0.4$ nm^{-1}, $d=6.0$ nm, and $V=0.52$ eV. For a specific $k_{\|}$, the spin polarization ratio increases in an oscillatory manner if the Dresselhaus SOC is enhanced. As a result, one can manipulate the SLSM-based SESS device by adjusting the strain, simultaneously meaning that a strain-controllable spin-polarized source can be achieved for semiconductor spintronics device applications.

Actually, the effective potential (U_{eff}) felt by an electron in the GaSb-based SLSM device still depends on semiconductor layer thickness (d) in addition to Dresselhaus SOC strength (η_D). Therefore, it is expected that the semiconductor layer thickness will affect the performance of the GaSb-based SLSM SESS device. Figure 5 shows that the spin polarization ratio (P_S) varies with electron energy (E) for semiconductor layer thickness $d=6.0$ nm (squares), 9.0 nm (circles) and 12.0 nm (stars), respectively, while other physical quantities are taken as $k_{\|}=0.4$ nm^{-1}, $\eta_D=0.187$ eV·nm^3, and $V=0.52$ eV. When the semiconductor layer thickness increases the spin polarization ratio obviously increases, and its magnitude and sign vary in an oscillatory manner with increasing electron energy. As a result, one can control this SESS device by appropriately fabricating the semiconductor layer thickness.

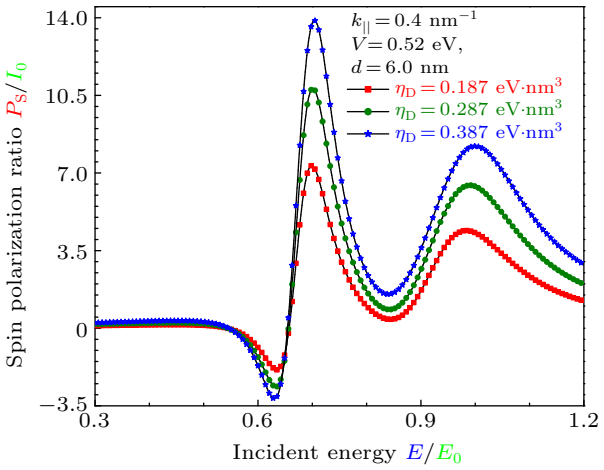


Fig. 4. Spin polarization ratio varies with the incident energy for Dresselhaus-SOC strength $\eta_D = 0.187$ eV·nm^3, 0.287 eV·nm^3, and 0.387 eV·nm^3, where other parameters are the same as those in Fig. 3.

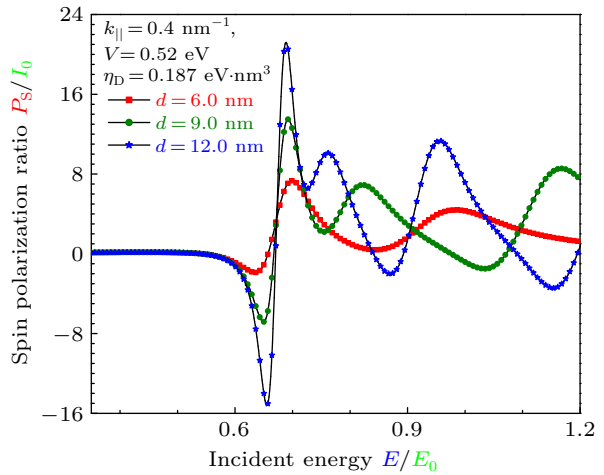


Fig. 5. Spin polarization ratio changes with incident energy for semiconductor-layer thickness $d=6.0$ nm, 9.0 nm, and 12.0 nm, where other parameters are the same as those in Fig. 4.

4. Conclusion

In conclusion, considering intrinsic Dresselhaus SOC in a GaSb-based SLSM, the GH effect of electrons is studied theoretically. We find that GH displacement for electrons across the GaSb-based SLSM depends evidently on spins because of Dresselhaus SOC. Thus, electron spins can be separated in the space dimension by spin-dependent GH shifts and the GaSb SLSM can act as a SESS device. We also find that this SESS device can be effectively manipulated by strain engineering

or semiconductor layer thickness, giving rise to a controllable spin-polarized source for semiconductor spintronics.

Acknowledgment

Project supported by the National Natural Science Foundation of China (Grant No. 62164005).

References

[1] Hossain M, Qin B, Li B and Duan X D 2022 *Nano Today* **42** 101338
[2] Linder J and Robinson J W A 2015 *Nat. Phys.* **11** 307
[3] Liu C S, Chen H W, Wang S Y, Liu Q, Jiang Y G, Zhang D W, Liu M and Zhou P 2020 *Nat. Nanotechnol.* **15** 545
[4] Gong C and Zhang X 2019 *Science* **363** 706
[5] Soumyanrayanan A, Reyren N, Fert A and Panagopoulos C 2016 *Nature* **539** 509
[6] Wroóbel J, Dietl T, Łusakowski A, Grabecki G, Fronc K, Hey R, Ploog K H and Shtrikman H 2004 *Phys. Rev. Lett.* **93** 246601
[7] Gurram M, Omar S and Wees B J V 2017 *Nat. Commun.* **8** 248
[8] Ohno Y, Young D K, Beschoten B, Matsukura F, Ohno H and Awschalom D D 1999 *Nature* **402** 790
[9] Li C L, Zhang J and Wang X M 2023 *Acta Phys. Sin.* **72** 227201 (in Chinese)
[10] Lu M W, Chen SY, Zhang G L and Huang X H 2018 *J. Phys. Condens. Matter* **30** 145302
[11] Wang L and Guo Y 2006 *Phys. Rev. B* **73** 205311
[12] Das S, Ghosh S, Kumar R, Bag A and Biswas D 2017 *IEEE Trans. Electron Dev.* **64** 4650
[13] Kang K, Lee K H, Han Y M, Gao H, Xie S E, Müller D A and Park J 2017 *Nature* **550** 229
[14] Zhao Y, Xie J, Zhang J and Hao Y 2014 *Appl. Phys. Lett.* **105** 223511
[15] Bindel J R, Pezzotta M, Ulrich J, Liebmamm M, Sheman E Y and Morgenstern M 2016 *Nat. Phys.* **12** 920
[16] Intronati G A, Tamborenea P I, Weinmann D A and Jarabert R A 2012 *Phys. Rev. Lett.* **108** 016601
[17] Kato Y, Myers R C, Gossard A C and Awschalom D D 2004 *Nature* **427** 50
[18] He Y P, Chen M X, Pan J F, Li D, Lin G J and Huang XH 2023 *Acta Phys. Sin.* **72** 028503 (in Chinese)
[19] Lu K Y, He Y P, He Z Y, Zu M M and Lu M W 2023 *IEEE Trans. Electron Dev.* **70** 1401
[20] Lu K Y, He Z Y, Zu M M and Guo S Y 2022 *IEEE Electron Device Lett.* **43** 1645
[21] Lu K Y, He Z Y, Zu M M, Guo S Y and Lu M W 2023 *IEEE Electron Device Lett.* **44** 1424
[22] Cao Z L, Lu M W, Huang X H, Guo Q M and Yang S Q 2020 *Superlattices Microstruct.* **143** 106545
[23] Cao Z L, Lu M W, Huang X H, Guo Q M and Yang S Q 2020 *J. Magn. Magn. Mater.* **513** 167217
[24] Cao Z L, Lu M W, Huang X H, Guo Q M and Yang S Q 2021 *J. Magn. Magn. Mater.* **527** 167785
[25] Cao Z L, Lu M W, Huang X H, Guo Q M and Yang S Q 2021 *Physica E* **129** 114646
[26] Cao X L, Chen SY, Huang X H, Guo Q M and Yang S Q 2022 *Vacuum* **206** 111541
[27] Xie S S, Lu M W, Chen S Y, Qin Y J, Wen L and Chen J J 2023 *Commun. Theor. Phys.* **75** 015703
[28] Chen X, Li C F and Ban Y 2008 *Phys. Rev. B* **77** 073307
[29] Trushin M and Schliemann J 2007 *New J. Phys.* **9** 346
[30] Rusetsky V S, Golyashov V A, Eremeev S V, Kusdov D A, Rusinov I P, Shamirzaev T S, Mironov A V, Demin A Y and Tereshchenko O E 2022 *Phys. Rev. Lett.* **129** 166802